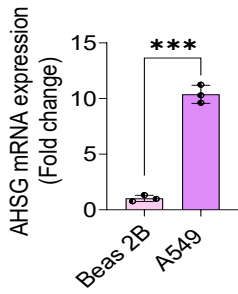


Supplementary File

Fig S1

A.



B.

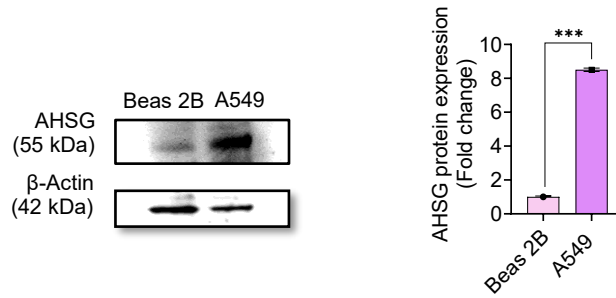


Fig. S1 AHSG is upregulated in LUAD. (A.) Relative mRNA expression showing the expression of AHSG in (BEAS-2B) vs. lung adenocarcinoma cells (A549). (B) Western blot analyses show the expression of AHSG in lung epithelial cells (BEAS-2B) vs. lung adenocarcinoma cells (A549 and H23) and its quantification. Data are presented as the mean \pm SD of three independent experiments. ($P < 0.05$; * $P < 0.01$; ** $P < 0.001$; ns, non-significant, compared with the normal group.) * $P < 0.05$ by Student's t-test.

Fig S2

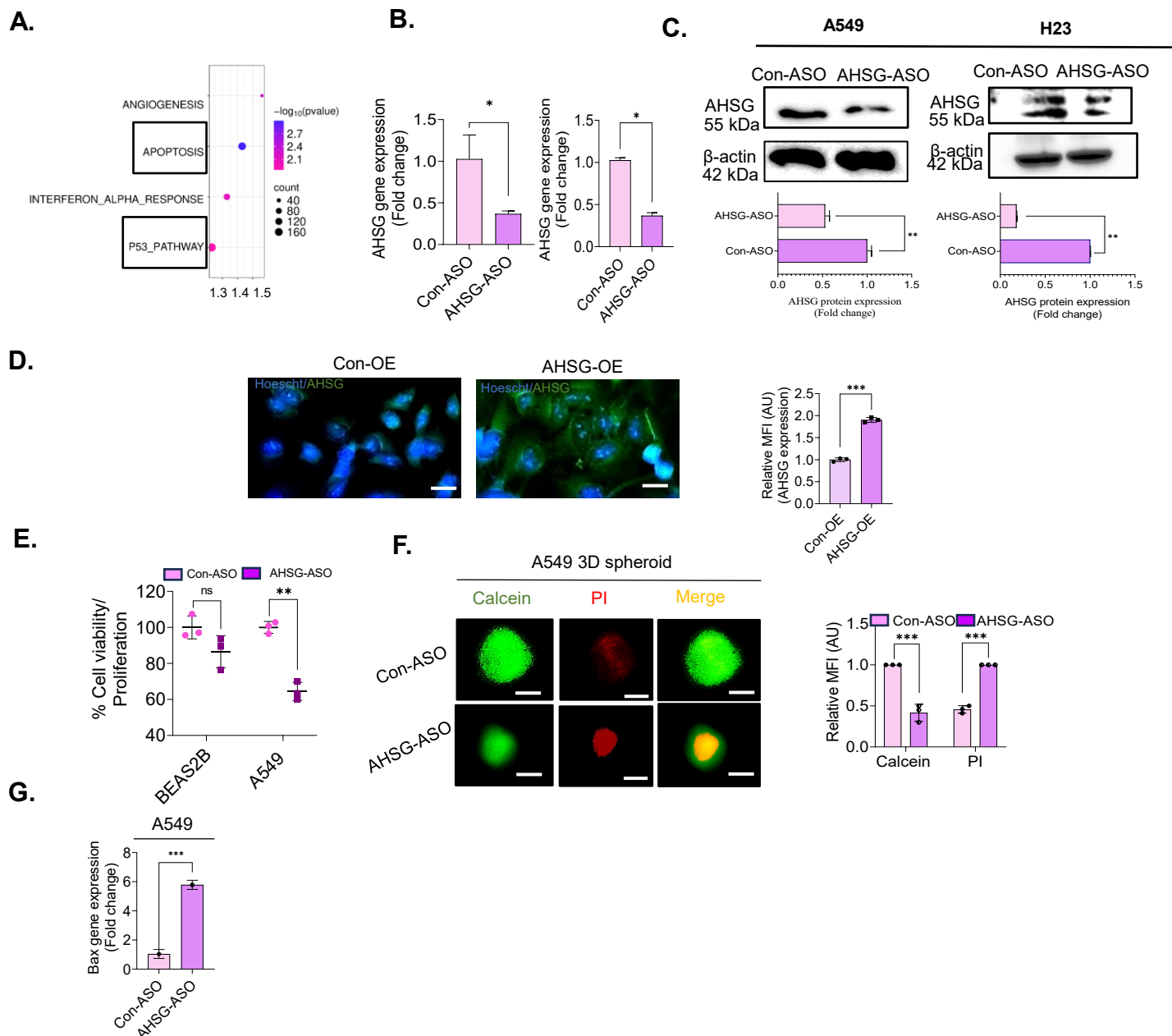
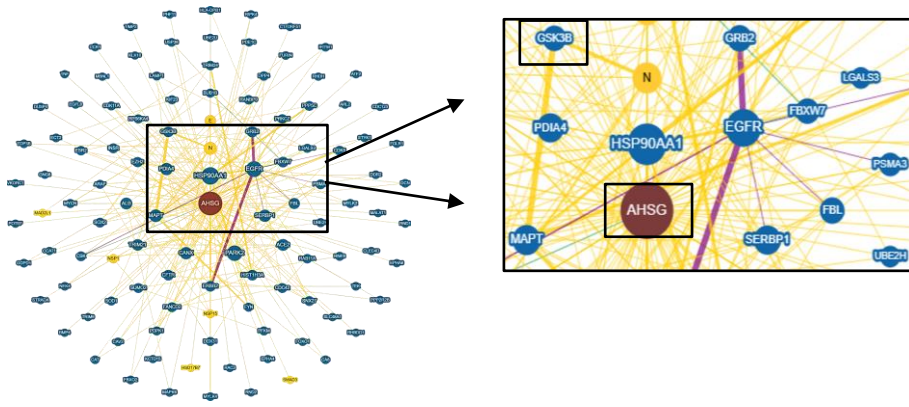


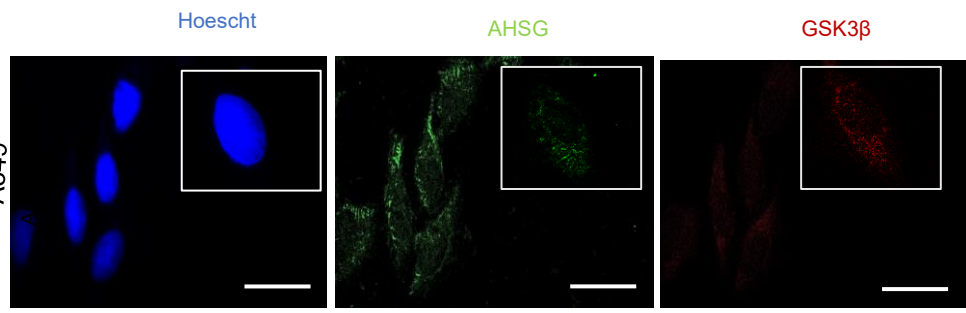
Fig. S2 AHSG promotes the proliferation of LUAD *in vitro* and promotes the viability of cancer cells. (A). Enrichment bubble RT-PCR and western blot confirmed the silencing efficiency of AHSG, along with its quantification in LUAD cells (A549 and H23) (B-C). (D). Immunofluorescence depicting AHSG expression in Con-OE and AHSG-OE (E). MTT depicting cell viability in BEAS2B and A549 cells (control and AHSG-ASO). (F). Calcein/PI staining and spheroid size determination of A549 3D unicellular tumor spheroids (Control and ASO) (objective 20X, scale bar 100 μ m). (G.) Bax gene expression in control and AHSG-ASO A549 cells. Data are presented as the mean \pm SD of three independent experiments. ($P < 0.05$; * $P < 0.01$; ** $P < 0.001$; ns, non-significant, compared with the normal group.)

Fig S3

A.



B.



C.

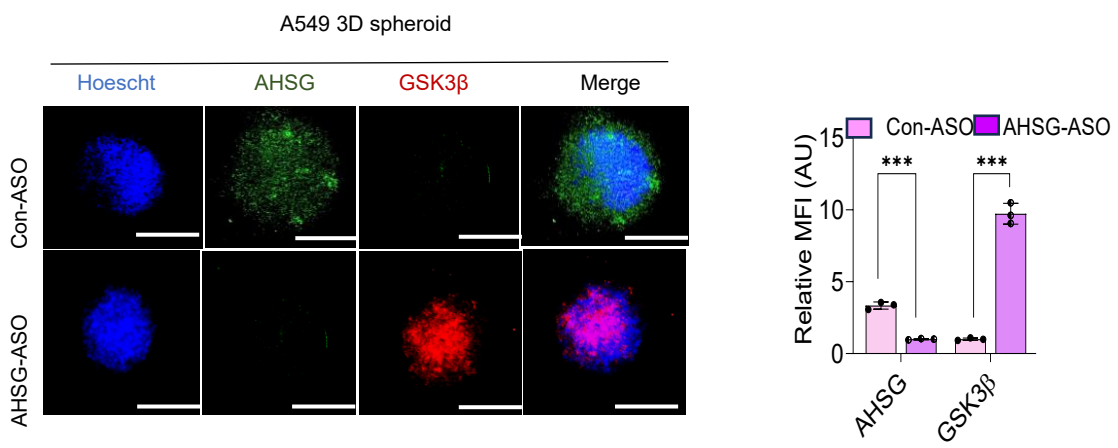


Fig. S3. AHSG interacts with GSK3β and results in its degradation.. (A).BioGRID demonstration of interactions (B). Immunofluorescent staining of the colocalization of AHSG and GSK3β. Pearson's coefficient was calculated to quantify the interactions between AHSG and GSK3β. (C.) Immunostaining of patient tissue sections and A549 3D spheroids.. Data are presented as the mean ± SD of three independent experiments. (P < 0.05; *P < 0.01; **P < 0.001; ns, non-significant, compared with the normal group.)